This article was downloaded by:
On: *23 January 2011*
Access details: *Access Details: Free Access*
Publisher *Taylor & Francis*
Informa Ltd Registered in England and Wales Registered Number: 1072954 Registered office: Mortimer House, 37-41 Mortimer Street, London W1T 3JH, UK

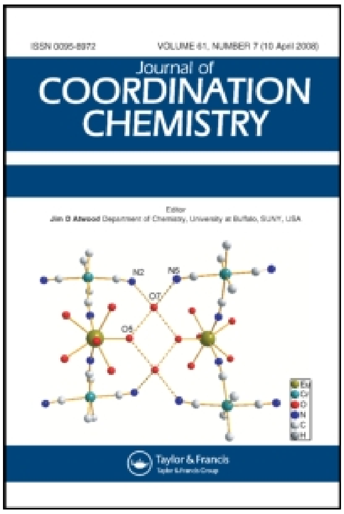

Journal of Coordination Chemistry

Publication details, including instructions for authors and subscription information:
http://www.informaworld.com/smpp/title~content=t713455674

Two inorganic chains based on the Anderson-type polyanions and transition metals

Peng-Peng Zhang[a]; Jun Peng[a]; Ai-Xiang Tian[a]; Hai-Jun Pang[a]; Yuan Chen[a]; Min Zhu[a]; Dan-Dan Wang[a]; Ming-Guan Liu[a]; Yong-Hui Wang[a]
[a] Key Laboratory of Polyoxometalate Science of Ministry of Education, Faculty of Chemistry, Northeast Normal University, Changchun, Jilin 130024, P.R. China

First published on: 14 September 2010

To cite this Article Zhang, Peng-Peng , Peng, Jun , Tian, Ai-Xiang , Pang, Hai-Jun , Chen, Yuan , Zhu, Min , Wang, Dan-Dan , Liu, Ming-Guan and Wang, Yong-Hui(2010) 'Two inorganic chains based on the Anderson-type polyanions and transition metals', Journal of Coordination Chemistry, 63: 20, 3610 — 3619, First published on: 14 September 2010 (iFirst)

To link to this Article: DOI: 10.1080/00958972.2010.516824

URL: http://dx.doi.org/10.1080/00958972.2010.516824

PLEASE SCROLL DOWN FOR ARTICLE

Full terms and conditions of use: http://www.informaworld.com/terms-and-conditions-of-access.pdf

This article may be used for research, teaching and private study purposes. Any substantial or systematic reproduction, re-distribution, re-selling, loan or sub-licensing, systematic supply or distribution in any form to anyone is expressly forbidden.

The publisher does not give any warranty express or implied or make any representation that the contents will be complete or accurate or up to date. The accuracy of any instructions, formulae and drug doses should be independently verified with primary sources. The publisher shall not be liable for any loss, actions, claims, proceedings, demand or costs or damages whatsoever or howsoever caused arising directly or indirectly in connection with or arising out of the use of this material.

Journal of Coordination Chemistry
Vol. 63, No. 20, 20 October 2010, 3610–3619

Taylor & Francis
Taylor & Francis Group

Two inorganic chains based on the Anderson-type polyanions and transition metals

PENG-PENG ZHANG, JUN PENG*, AI-XIANG TIAN, HAI-JUN PANG,
YUAN CHEN, MIN ZHU, DAN-DAN WANG,
MING-GUAN LIU and YONG-HUI WANG

Key Laboratory of Polyoxometalate Science of Ministry of Education, Faculty of
Chemistry, Northeast Normal University, Changchun, Jilin 130024, P.R. China

(*Received 8 March 2010; in final form 16 July 2010*)

Two new compounds based on Anderson-type polyanions, $H(C_6H_9N_3O_2)_2[Mn(H_2O)_2][Al(OH)_6Mo_6O_{18}] \cdot 6H_2O$ (**1**) and $(C_6H_{10}N_3O_2)_2[Ag(H_2O)_2][Cr(OH)_6Mo_6O_{18}] \cdot 6H_2O$ (**2**), have been synthesized in aqueous solution and characterized by elemental analyses, IR, TG, and single crystal X-ray diffraction. Both compounds show inorganic 1-D chain-like structures in which the Anderson-type polyanions are bidentate ligands chelating to two metal cations. Further, transition metal cations are in the same line with the center Al (Cr), which is unusual in 1-D inorganic chains based on Anderson-type polyanions. Free histidine molecules further link the chains into 3-D supramolecular frameworks *via* hydrogen interactions. Electrochemical and fluorescence quenching properties were investigated.

Keywords: Anderson-type polyanion; Inorganic chain; Transition metals

1. Introduction

Design and synthesis of materials based on polyoxometalates (POMs) are developing rapidly due to their various topologies and applications in fields as diverse as catalysis, magnetism, medicine, optics, and electrochemistry [1–5]. With abundant oxygens on the surface and high negative charges, POMs are usually chosen as inorganic O-donors to assemble with metal cations or metal–organic frameworks to construct POM-based materials [6–10]. POM-based inorganic materials often exhibit many topologies and applications and have attracted much interest [11–19]. One strategy to construct such materials is adopting appropriate metal linkers to connect discrete POM units into 1-D, 2-D, and 3-D extended inorganic solid frameworks. Most of such materials are based on lanthanide linkers due to their highly oxophilic characteristics and multiple coordination numbers [20–23]. However, transition metal (TM) cations exhibit more coordination modes than lanthanides. Furthermore, catalytic and magnetic properties

---

*Corresponding author. Email: jpeng@nenu.edu.cn

Journal of Coordination Chemistry
ISSN 0095-8972 print/ISSN 1029-0389 online
DOI: 10.1080/00958972.2010.516824

of TM cations could be utilized. So, it is significant to construct POM-based inorganic materials with TM linkers.

Anderson-type polyanions with planar structure is one of the most important species of POMs. In this type of structure, each metal (Mo or W) has two terminal oxygens, which make the polyanion highly reactive to TMs [24–32]. However, compounds based on Anderson-type polyanions are relatively less than other POMs, such as Keggin [33], Wells–Dawson [34], and Lindquist-type [35]. Therefore, it is promising to design and synthesize compounds based on Anderson-type polyanions.

Here, we report two new compounds, $H(C_6H_9N_3O_2)_2[Mn(H_2O)_2][Al(OH)_6Mo_6O_{18}] \cdot 6H_2O$ (**1**) and $(C_6H_{10}N_3O_2)_2[Ag(H_2O)_2][Cr(OH)_6Mo_6O_{18}] \cdot 6H_2O$ (**2**), with Anderson-type polyanions and TM cations. Both compounds show 1-D inorganic chain-like structures, in which the Anderson-type polyanions are linked by Mn^{II} and Ag^{I}. Such structures constructed from Anderson-type polyanions and TM cations are few [36–38]. In these two compounds, the Anderson-type polyanions are bidentate, chelating to two metal cations. Further, the TM cations situate in the same line with the center Al (Cr), which is unusual in 1-D inorganic chains based on Anderson-type polyanions.

2. Experimental

2.1. *Materials and general procedures*

All reagents were purchased commercially and used without purification. Elemental analyses (C, H, and N) were performed on a Perkin Elmer 2400 CHN Elemental Analyzer. IR spectra were obtained on an Alpha Centaurt FT-IR spectrometer with KBr pellets in the range 400–4000 cm^{-1}. Thermal gravimetric analyses (TGA) were carried out on a Perkin Elmer TGA7 instrument in flowing N_2 with a heating rate of $10^{\circ}C\,min^{-1}$. X-ray powder diffraction (XRPD) patterns were recorded on a Siemens D5005 diffractometer with Cu-Kα ($\lambda = 1.5418$ Å) radiation.

2.2. *Synthesis of $H(C_6H_9N_3O_2)_2[Mn(H_2O)_2][Al(OH)_6Mo_6O_{18}] \cdot 6H_2O$ (1)*

0.1 g $AlCl_3 \cdot 6H_2O$ (0.8 mmol) was dissolved in 10 mL of distilled water, into which a 10 mL aqueous solution containing 0.36 g $Na_2MoO_4 \cdot 2H_2O$ (1.5 mmol) and then 2 mL of glacial acetic acid were added with stirring at room temperature (**A**). 0.1 g $Mn(CH_3COO)_2 \cdot 4H_2O$ (0.5 mmol) in 5 mL water was added to 5 mL solution containing 0.155 g histidine ($C_6H_9N_3O_2$, 1 mmol) (**B**). Then, solution **B** was added dropwise to solution **A**. The final pH was adjusted to 2.6 with concentrated HCl, and the solution was heated for 10 min. The filtrate was kept for 1 week at room temperature, and then yellow block crystals of **1** were collected in 45% yield (based on Mn). $C_{12}H_{41}N_6MnO_{36}AlMo_6$ (1503.0324): Calcd: C, 9.59%; H, 2.75%; and N, 5.59%. Found: C, 9.52%; H, 2.81%; and N, 5.54%. IR (solid KBr pellet, cm^{-1}): 3384(w), 3134(w), 1614(s), 1505(m), 1391(s), 1335(w), 1163(w), 1082(w), 945(s), 913(s), 859(w), 650(s), 563(w), and 445(w).

2.3. *Synthesis of* $(C_6H_{10}N_3O_2)_2[Ag(H_2O)_2][Cr(OH)_6Mo_6O_{18}]\cdot 6H_2O$ *(2)*

Compound **2** is prepared in a way similar to **1**, except using $Cr(NO_3)_3\cdot 6H_2O$ and $AgNO_3$ instead of $AlCl_3\cdot 6H_2O$ and $Mn(CH_3COO)_2\cdot 4H_2O$. Pink block crystals; yield 47% (based on Ag). $C_{12}H_{42}N_6AgO_{36}CrMo_6$ (1581.9850): Calcd: C, 9.11%; H, 2.68%; and N, 5.31%. Found: C, 9.12%; H, 2.71%; and N, 5.34%. IR (solid KBr pellet, cm^{-1}): 3134(w), 3029(w), 2005(w), 1623(s), 1578(w), 1509(m), 1396(s), 1341(w), 1268(w), 1182(w), 1091(w), 945(s), 909(s), 804(w), 654(s), 568(w), and 445(m).

2.4. *Preparation of 1- and 2-carbon paste electrodes*

The **1**-carbon paste electrode (CPE) was fabricated as follows: 96 mg of graphite powder and 8 mg of **1** were mixed and ground together by agate mortar and pestle to achieve a uniform mixture, and then 0.6 mL of nujol was added with stirring. The homogenized mixture was packed into a glass tube with a 1.2 mm inner diameter, and the tube surface was wiped with paper. Electrical contact was established with a copper rod through the back of the electrode. In a similar manner, **2**-CPE electrode was made with **2**.

2.5. *X-ray crystallography*

Crystal data for the two compound**s** were collected on a Bruker SMART-CCD diffractometer with Mo-Kα monochromatic radiation. The structures were solved by direct methods and refined by full-matrix least-squares on F^2 using the SHELXTL crystallographic software package [39, 40]. Crystallographic data of the compounds are summarized in table 1.

3. Results and discussion

Compounds **1** and **2** were synthesized in aqueous solution. The manganese cations in **1** are in +2 oxidation state and the silver cations in **2** are +1 oxidation state, confirmed by charge balance, coordination environments and bond valence sum (BVS) calculations [41]. All Mo ions are of +6 oxidation state; Al and Cr are of +3 oxidation state. Furthermore, one and two protons are added to histidine for charge balance, similar to reported cases [42, 43]. So, the compounds are formulated as $H(C_6H_9N_3O_2)_2[Mn(H_2O)_2][Al(OH)_6Mo_6O_{18}]\cdot 6H_2O$ (**1**) and $(C_6H_{10}N_3O_2)_2[Ag(H_2O)_2][Cr(OH)_6Mo_6O_{18}]\cdot 6H_2O$ (**2**).

3.1. *Description of the structures*

Single-crystal structural analyses reveal that **1** and **2** are isomorphous; therefore, the structure of **1** is described here representatively.

Compound **1** is built up from one Anderson-type polyoxoanion $[Al(OH)_6Mo_6O_{18}]^{3-}$, one Mn^{II}, two histidine molecules, and eight waters (figure 1).

Table 1. Crystal data and structure refinement for **1** and **2**.

Compounds	**1**	**2**
Empirical formula	$C_{12}H_{41}N_6MnO_{36}AlMo_6$	$C_{12}H_{42}N_6AgO_{36}CrMo_6$
Mr	1503.07	1582.03
Color, habit	Yellow, block	Pink, block
Crystal size (mm^3)	$0.149 \times 0.117 \times 0.1$	$0.168 \times 0.142 \times 0.119$
Temperature (K)	293(2)	293(2)
Wavelength (Å)	0.71069	0.71069
Crystal system	Triclinic	Triclinic
Space group	$P\bar{1}$	$P\bar{1}$
Unit cell dimensions (Å, °)		
a	9.3980(11)	9.5020(13)
b	10.8330(13)	10.9120(15)
c	11.6600(14)	11.4970(15)
α	67.7510(14)	66.9470(16)
β	69.9520(14)	71.0150(16)
γ	68.8140(16)	70.0020(16)
V (Å^3)	994.8(2)	1005.2(2)
Z	1	1
D_{Calcd} (g cm^{-3})	2.507	2.613
μ (Mo-Kα) (cm^{-1})	2.282	2.665
$F(000)$	732.0	767
hkl range	$-11 \le h \le 9$; $-13 \le k \le 13$; $-14 \le l \le 9$	$-11 \le h \le 10$; $-13 \le k \le 13$; $-14 \le l \le 13$
Reflections measured	5405	6173
Reflections unique	3809	3836
R_{int}	0.0200	0.0194
Reflections parameters	290	304
Final R indices [$I > 2\sigma(I)$]	$R_1{}^a = 0.0644$, $wR_2{}^b = 0.1667$	$R_1{}^a = 0.0593$, $wR_2{}^b = 0.1488$
Goodness-of-fit (F^2)^a	1.043	1.105
$\Delta\rho_{\mathrm{fin}}$ (max/min) (e Å^{-3})	1.828/−3.828	1.158/−1.360

$^aR_1 = \sum||F_o| - |F_c||/\sum|F_o|$; $^bwR_2 = \{\sum[w(F_o^2 - F_c^2)^2]/\sum[w(F_o^2)^2]\}^{1/2}$.

The polyoxoanion $[Al(OH)_6Mo_6O_{18}]^{3-}$ belongs to the B-type Anderson structure, which consists of seven edge-shared octahedra, six of which are Mo octahedra, arranged hexagonally around the central Al octahedron. The Mo ions form approximately a regular planar hexagonal configuration encircling the Al center. The difference Fourier maps indicate that the six μ_3-bridging oxygens around Al^{3+} are protonated [44]. The molybdenum–oxygen distances in **1** can be grouped into three sets: Mo–O_t (terminal oxygen), Mo–O_b (bridging oxygen), and Mo–O_c (central oxygen common to two molybdenums and aluminum). Selected bond distances (Å) and angles (°) for **1** and **2** are listed in table S1. All bond lengths and angles are within normal ranges, consistent with those described in the literature [24, 25].

In the structure, each Anderson-type polyanion is bidentate chelating to two Mn^{II} *via* four terminal oxygens. The Mn^{II} is octahedral coordinated by four oxygens from two Anderson polyanions and two waters. The Mn^{II} cations situate in the same line with the center Al, unusual in 1-D inorganic chains based on Anderson-type polyanions. The bond lengths around Mn^{II} are 2.153(8) Å (Mn–O12), 2.159(10) Å (Mn–OW1), and 2.330(10) Å (Mn–O7), and the bond angles are 87.9(4)–92.1(4)° (O–Mn–O). The Anderson-type polyanions and Mn^{II} cations arrange alternately to form a 1-D inorganic chain, as shown in figure 2.

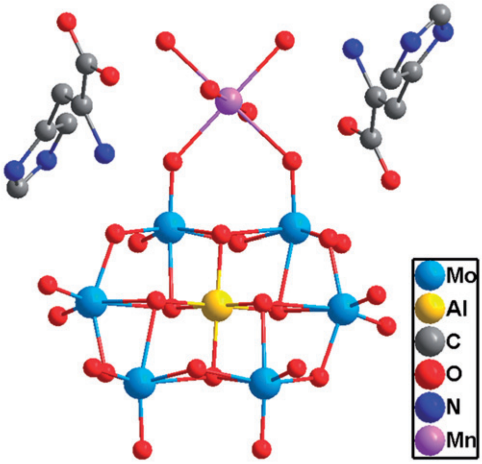

Figure 1. Stick–ball view of the asymmetric unit of **1**. The hydrogens and lattice waters are omitted for clarity.

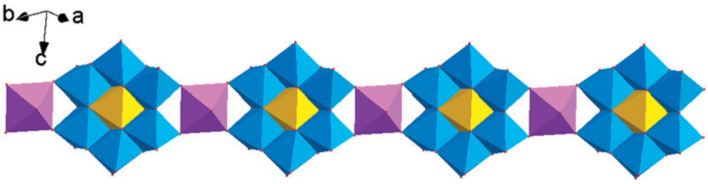

Figure 2. The 1-D inorganic chain of **1**.

In addition, free histidines locate in the space among the inorganic chains. Through hydrogen bonding interactions, histidine and oxygen from the polyanions form a 16-membered supramolecular ring (figure 3). The Anderson-type polyanions and supramolecular rings array side by side to form a supramolecular chain, and then they cross with the 1-D inorganic chains to form a 3-D supramolecular framework (figure 4). Hydrogen bonding parameters in **1** are in table 2. The lattice waters further reinforce the whole structure.

3.2. *IR spectroscopy and XRPD patterns*

Spectra of the two compounds are very similar in the given region (figure S1). Bands at 1082–1614 cm^{-1} and 1091–1623 cm^{-1} are characteristic of histidine molecules; 936, 904, 859, 800, 646, 563, and 445 cm^{-1} in **1** and 945, 909, 804, 654, 568, and 445 cm^{-1} in **2** are ascribed to the Anderson-type polyanions.

The XRPD patterns for **1** and **2** are presented in figure S2. The diffraction peaks of the simulated and experimental patterns match well, indicating phase purity of the two compounds.

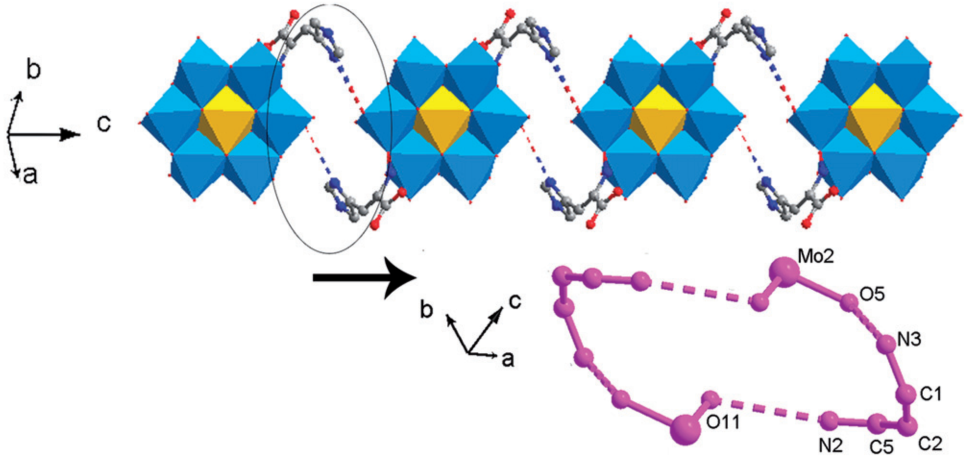

Figure 3. The supramolecular chain is built up by histidine molecules and the Anderson-type polyanions. The 16-membered supramolecular ring is shown in purple.

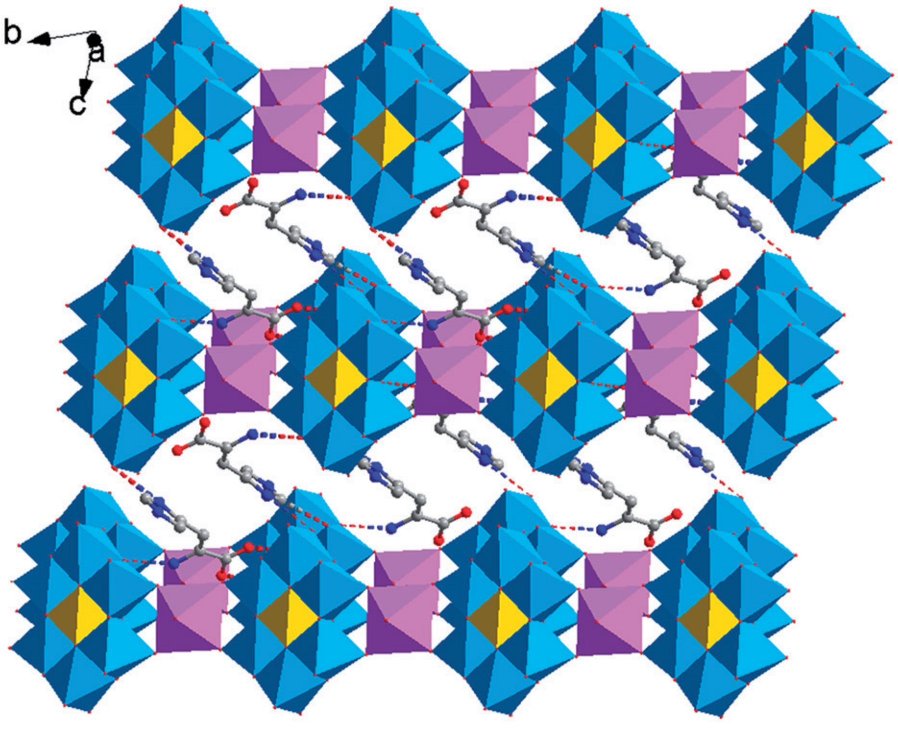

Figure 4. The hydrogen bonds around the 1-D chains and histidine molecules in the 3-D supramolecular framework of **1**. The hydrogens are omitted for clarity. (The hydrogen bonds are shown in dashed lines.)

Table 2. Hydrogen bonding parameters in **1**.

D–H···A	D–H	H···A	D···A	∠(DHA)
O1–H3···O13	0.86(16)	1.90(15)	2.751(14)	172(14)
O10–H1···O14(i)	0.76(14)	1.84(15)	2.601(14)	172(25)
N3–H3B···O13(ii)	0.86	2.48	3.016(16)	121
N3–H3A···O5(ii)	0.86	1.89	2.748(16)	172
O13–H13A···O1	0.85	1.92	2.751(19)	107
C3–H8···O3(iii)	0.93	2.07	2.87(2)	144

Symmetry coordinates for **1**: (i) $-x+1, -y-2, -z+1$; (ii) $-x+1, -y-1, -z+1$; (iii) $x+1, y+1, z-1$.

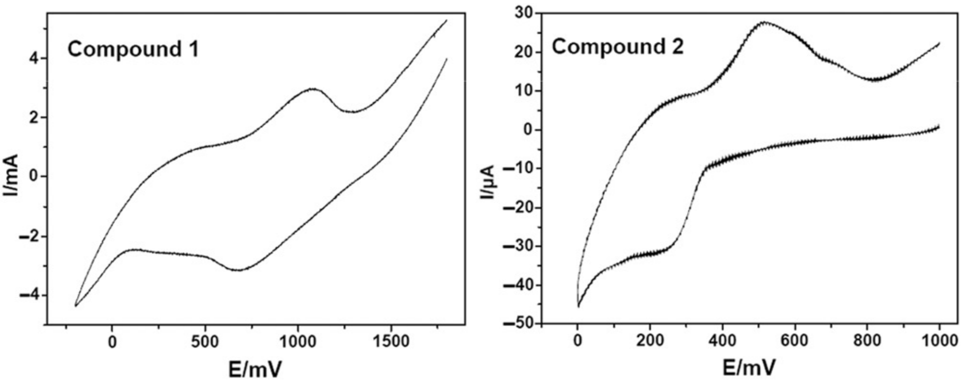

Figure 5. The cyclic voltammograms of **1**- and **2**-CPEs in $1\,\mathrm{mol\,L^{-1}}$ H_2SO_4 solution.

3.3. *Thermal analyses*

The TGA also supports the chemical compositions of **1** and **2** (figure S3). The TG curve of **1** shows a total weight loss of 34.99% at 50–500°C, which agrees with the calculated value of 34.43%. The first weight loss of 9.61% (Calcd 9.59%) under 200°C may be assigned to removal of all water. The weight loss from 200°C to 500°C of 25.38% (Calcd 24.84%) may be ascribed to decomposition of the organic molecules and the polyanions. Compound **2** exhibits similar TG curve as **1** with total weight loss of 33.04% (Calcd 33.28%), the first loss of 9.10 (Calcd 9.27%) and the second loss of 23.94% (Calcd 24.04%).

3.4. *Cyclic voltammetry*

Because these two compounds are insoluble in aqueous solution and common organic solvents, they are optimal choices for use in bulk-modified CPE method to study their electrochemical properties [45]. The electrochemical behaviors were studied in $1\,\mathrm{mol\,L^{-1}}$ H_2SO_4 aqueous solution (figure 5). Both CPEs show a pair of redox peaks, attributed to Mn^{II}/Mn^{III} (1081.2 and 677.6 mV) and Ag^0/Ag^+ (512.0 and 256.6 mV) couples, respectively [46, 47]. The mean peak potentials ($E_{1/2}=(E_{pa}+E_{pc})/2$) are 879.4 and 384.3 mV.

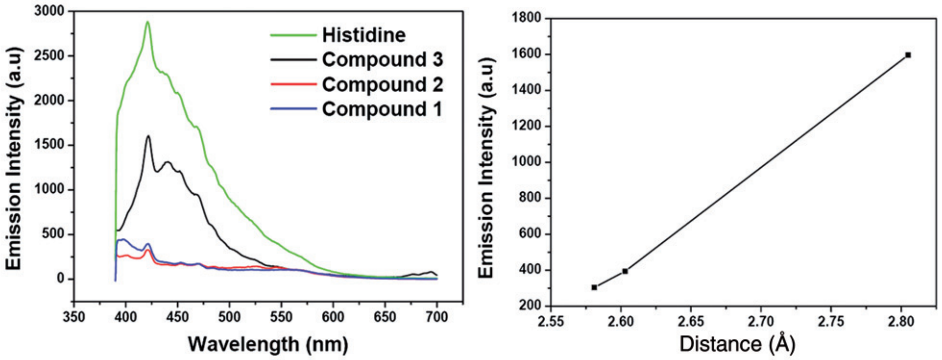

Figure 6. Left: Solid-state emission spectra of free histidine and **1**–**3** at room temperature. Right: Plot of the nearest distance between the polyanion and histidine *vs*. fluorescence quenching degree for **1**–**3**.

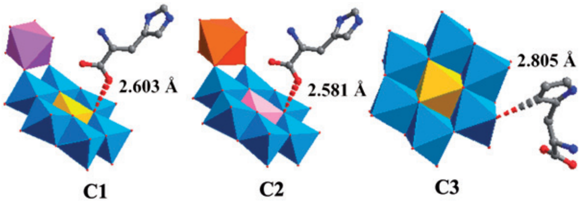

Figure 7. The nearest distances between the polyanion and the histidine in **1**–**3**.

3.5. *Fluorescence quenching*

Fluorescence quenchers are widely used in analysis, medicine, etc. [48–50]. POMs often exhibit fluorescence quenching toward many substances [51, 52]. Here, the solid-state photoluminescence properties of **1** and **2** at room temperature were investigated (figure 6, left). As a contrast, photoluminescence properties of free histidine and histidine compounds of Anderson-type POM (**3**, [53]) were studied simultaneously. These four spectra show emission maxima at *ca* 421 nm upon excitation at 365 nm, which means that the luminescence of the compounds can be attributed to histidine emission. The POM-based compounds could act as quenchers to decrease the fluorescence intensity of histidine; the fluorescence intensities decrease in the order **2** > **1** > **3**. The nearest distances between histidine molecules and polyanions are 2.603 Å in **1**, 2.581 Å in **2**, and 2.804 Å in **3**, parallel with their fluorescence quenching (figure 7). This means that the shorter the distance between polyanion and histidine, the higher the fluorescence quenching (figure 6, right). The main interactions between polyanions and histidine in the compounds are H-bonding; so the distances between the two parts should play the key role in the fluorescence quench process.

4. Conclusions

Two new compounds based on Anderson-type polyanions have been obtained. Both show inorganic chain-like structures with Mn^{II} and Ag^{I} as linkers. Histidines connect the chains to form a 3-D supramolecular structure through hydrogen bonds. These two compounds enrich the family of the Anderson-type polyanions. Further, this approach is significant in the area of constructing POM-based inorganic materials.

Supplementary materials

Supplementary data associated with this article: the IR, XRPD, and TG curves of the title compounds. Crystallographic data for the structures reported in this article have been deposited in the Cambridge Crystallographic Data Center with CCDC nos of 735768 and 755271.

Acknowledgments

This study was financially supported by the National Science Foundation of China (20671016) and by the analysis and testing foundation of Northeast Normal University.

References

[1] C.Y. Sun, S.X. Liu, D.D. Liang, K.Z. Shao, Y.H. Ren, Z.M. Su. *J. Am. Chem. Soc.*, **131**, 1883 (2009).
[2] A. Müller, F. Peters. *Chem. Rev.*, **98**, 239 (1998).
[3] J.T. Rhule, C.L. Hill, D.A. Judd. *Chem. Rev.*, **98**, 327 (1998).
[4] T. Yamase. *J. Chem. Soc., Dalton Trans.*, 2585 (1985).
[5] E. Coronado, C. Giménez-Saiz, C.J. Gómez-García. *Coord. Chem. Rev.*, **249**, 1776 (2005).
[6] Y.W. Li, Y.H. Wang, Y.G. Li, E.B. Wang, W.L. Chen, Q. Wu, Q. Shi. *Inorg. Chim. Acta*, **362**, 1078 (2009).
[7] J.Q. Sha, J. Peng, H.S. Liu, J. Chen, B.X. Dong, A.X. Tian, Z.M. Su. *Eur. J. Inorg. Chem.*, 1268 (2007).
[8] B.X. Dong, J. Peng, C.J. Gómez-García, S. Benmansour, H.Q. Jia, N.H. Hu. *Inorg. Chem.*, **46**, 5933 (2007).
[9] A.X. Tian, J. Ying, J. Peng, J.Q. Sha, Z.G. Han, J.F. Ma, Z.M. Su, N.H. Hu, H.Q. Jia. *Inorg. Chem.*, **47**, 3274 (2008).
[10] C. Qin, X.L. Wang, E.B. Wang, Z.M. Su. *Inorg. Chem.*, **47**, 555 (2008).
[11] W.L. Chen, Y.G. Li, Y.H. Wang, E.B. Wang. *Eur. J. Inorg. Chem.*, 2216 (2007).
[12] H.Q. Tan, W.L. Chen, Y.G. Li, D. Liu, L.M. Chen, E.B. Wang. *J. Solid State Chem.*, **182**, 465 (2009).
[13] H.Q. Tan, Y.G. Li, Z.M. Zhang, C. Qin, X.L. Wang, E.B. Wang, Z.M. Su. *J. Am. Chem. Soc.*, **129**, 10066 (2007).
[14] L.H. Fan, L. Xu, G.G. Gao, F.Y. Li, Z.K. Li, Y.F. Qiu. *Inorg. Chem. Commun.*, **9**, 1308 (2006).
[15] Z.M. Zhang, Y.G. Li, W.L. Chen, E.B. Wang, X.L. Wang. *Inorg. Chem. Commun.*, **11**, 879 (2008).
[16] H. Imai, T. Akutagawa, F. Kudo, M. Ito, K. Toyoda, S. Noro, L. Cronin, T. Nakamura. *J. Am. Chem. Soc.*, **131**, 13578 (2009).
[17] (a) C. Ritchie, C. Streb, J. Thiel, S.G. Mitchell, H.N. Miras, D.L. Long, T. Boyd, R.D. Peacock, T. McGlone, L. Cronin. *Angew. Chem.*, **120**, 6987 (2008); (b) *Angew. Chem. Int. Ed.*, **47**, 6881 (2008).
[18] (a) C. Streb, C. Ritchie, D.L. Long, P. Kögerler, L. Cronin. *Angew. Chem.*, **119**, 7723 (2007); (b) *Angew. Chem. Int. Ed.*, **46**, 7579 (2007).
[19] J. Thiel, C. Ritchie, C. Streb, D.L. Long, L. Cronin. *J. Am. Chem. Soc.*, **131**, 4180 (2009).
[20] C.D. Wu, C.Z. Lu, H.H. Zhuang, J.S. Huang. *J. Am. Chem. Soc.*, **124**, 3836 (2002).
[21] J.P. Wang, X.Y. Duan, X.D. Du, J.Y. Niu. *Cryst. Growth Des.*, **6**, 2266 (2006).
[22] X.Y. Zhao, S.X. Liu, Y.H. Ren, J.F. Cao, R.G. Cao, K.Z. Shao. *J. Solid State Chem.*, **181**, 2488 (2008).
[23] Y. Lu, Y. Xu, Y.G. Li, E.B. Wang, X.X. Xu, Y. Ma. *Inorg. Chem.*, **45**, 2055 (2006).
[24] V. Shivaiah, M. Nagaraju, S.K. Das. *Inorg. Chem.*, **42**, 6604 (2003).
[25] V. Shivaiah, S.K. Das. *Inorg. Chem.*, **44**, 8846 (2005).

[26] C. Martin, C. Lamonier, M. Fournier, O. Mentré, V. Harlé, D. Guillaume, E. Payen. *Inorg. Chem.*, **43**, 4636 (2004).
[27] A.M. Khenkin, R. Neumann. *Adv. Synth. Catal.*, **344**, 1017 (2002).
[28] R.G. Cao, S.X. Liu, L.H. Xie, Y.B. Pan, J.F. Cao, Y.H. Ren, L. Xu. *Inorg. Chem.*, **46**, 3541 (2007).
[29] H.Y. An, Z.B. Han, T.Q. Xu, C.G. Meng, E.B. Wang. *Inorg. Chem. Commun.*, **11**, 914 (2008).
[30] V. Shivaiah, P.V.N. Reddy, L. Cronin, S.K. Das. *J. Chem. Soc., Dalton Trans.*, 3781 (2002).
[31] B. Gao, S.-X. Liu, C.-D. Zhang, L.-H. Xie, C.-Y. Sun, M. Yu. *J. Coord. Chem.*, **60**, 911 (2007).
[32] J.P. Wang, S.Z. Li, J.Y. Niu. *J. Coord. Chem.*, **60**, 1327 (2007).
[33] A.X. Tian, J. Ying, J. Peng, J.Q. Sha, H.J. Pang, P.P. Zhang, Y. Chen, M. Zhu, Z.M. Su. *Cryst. Growth Des.*, **8**, 3717 (2008).
[34] J.Q. Sha, J. Peng, Y.Q. Lan, Z.M. Su, H.J. Pang, A.X. Tian, P.P. Zhang, M. Zhu. *Inorg. Chem.*, **47**, 5145 (2008).
[35] E.F. Wilson, H. Abbas, B.J. Duncombe, C. Streb, D.L. Long, L. Cronin. *J. Am. Chem. Soc.*, **130**, 13876 (2008).
[36] H.Y. An, Y.G. Li, D.R. Xiao, E.B. Wang, C.Y. Sun. *Cryst. Growth Des.*, **6**, 1107 (2006).
[37] H.Y. An, T.Q. Xu, C.Y. Jia, H. Zheng, W.S. Mu. *J. Mol. Struct.*, **933**, 86 (2009).
[38] B. Gao, S.X. Liu, L.H. Xie, M. Yu, C.D. Zhang, C.Y. Sun, H.Y. Cheng. *J. Solid State Chem.*, **179**, 1681 (2006).
[39] G.M. Sheldrick. *SHELX-97*, *Program for Crystal Structure Refinement*, University of Göttingen, Germany (1997).
[40] G.M. Sheldrick. *SHELXL-97*, *Program for Crystal Structure Solution*, University of Göttingen, Germany (1997).
[41] I.D. Brown, D. Altermatt. *Acta Crystallogr.*, **41B**, 244 (1985).
[42] H.Y. An, Y.G. Li, E.B. Wang, D.R. Xiao, C.Y. Sun, L. Xu. *Inorg. Chem.*, **44**, 6062 (2005).
[43] J. Liu, Y.G. Li, E.B. Wang, D.R. Xiao, L.L. Fan, Z.M. Zhang, Y. Wang. *J. Mol. Struct.*, **837**, 237 (2007).
[44] D. Honda, S. Ikegami, T. Inoue, T. Ozeki, A. Yagasaki. *Inorg. Chem.*, **46**, 1464 (2007).
[45] C.Y. Sun, S.X. Liu, L.H. Xie, C.L. Wang, B. Gao, C.D. Zhang, Z.M. Su. *J. Solid State Chem.*, **179**, 2093 (2006).
[46] B. Li, Y. Yan, F.Y. Li, L. Xu, L.H. Bi, L.X. Wu. *Inorg. Chim. Acta*, **362**, 2796 (2009).
[47] G.G. Gao, P.S. Cheng, T.C.W. Mak. *J. Am. Chem. Soc.*, **131**, 18257 (2009).
[48] M.M. Puchalskl, M.J. Morra. *Environ. Sci. Technol.*, **26**, 1787 (1992).
[49] K.N. Kim, Y.W. Kwon, D.H. Choi, J.I. Jin. *Macromol. Chem. Phys.*, **210**, 1372 (2009).
[50] X.W. Zhuang, T. Ha, H.D. Kim, T. Centner, S. Labeit, S. Chu. *Biophysics*, **97**, 14241 (2000).
[51] Y.F. Qiu, L. Xu, G.G. Gao, W.J. Wang, F.Y. Li. *Inorg. Chim. Acta*, **359**, 451 (2006).
[52] H.M. Zhang, Y.Q. Wang, Q.H. Zhou, G.L. Wang. *J. Mol. Struct.*, **921**, 156 (2009).
[53] Crystal data for compound **3**: $C_{12}H_{43}N_6AlMo_6O_{36}$, $Fw=1450.11$, Triclinic, space group $P1$, $a=9.0495(18)$ Å, $b=10.513(2)$ Å, $c=12.124(2)$ Å, $\alpha=100.975(3)^\circ$, $\beta=111.852(3)^\circ$, $\gamma=98.625(3)^\circ$, $V=1019.6(4)$ Å^3, $Z=1$, $D_{\mathrm{Calcd}}=2.317\,\mathrm{Mg\,m^{-3}}$, $\lambda=0.71073$ Å, $T=293(2)$ K, $R_1(wR_2)=0.0335$ (0.0919), Bruker Smart Apex-II CCD area detector, Mo-Kα radiation. The structure was solved by direct methods and refined on F^2 by full-matrix least-squares methods using SHELXTL 97.